

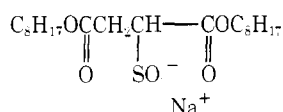
Adsorption, Displacement, and Ionization in Water Pools

F. M. Menger* and G. Saito

Contribution from the Department of Chemistry, Emory University, Atlanta, Georgia 30322. Received December 27, 1977

Abstract: *p*-Nitrophenol experiences a 4.5 pK_a unit increase when solubilized into AOT-stabilized water pools containing inorganic buffers. This is attributed to adsorption at the pool interface where phenolic hydroxyls are held in proximity to anionic surfactant groups. Unfavorable desorption equilibria precede ionization. When excess imidazole (but not methanol or *n*-butyl alcohol) is added to a pool, a fraction of the interfacial *p*-nitrophenol is displaced into the pool water (the fraction depending on the amount of imidazole). The portion of the phenol in the aqueous environment has a pK_a much closer to that in bulk water (7.5–7.9 depending on the imidazole concentration). Relative amounts of the “low pK_a ” and “high pK_a ” phenol in the imidazole-buffered pools depend on the pool size (controlled by the ratio of water to surfactant in the heptane). On the other hand, the acidity of pool-incorporated *p*-nitrophenol is not sensitive to pool size within the range investigated. These results are compared with acid–base equilibria on protein surfaces.

In 1973 we coined the term “water pool” to describe inverted micelles containing large amounts of water.¹ Water pools are formed in aprotic solvents by a variety of surfactants such as di-2-ethylhexylsodium sulfosuccinate (called commercially Aerosol OT or AOT). When this salt dissolves in hydrocarbon solvents, it aggregates into micelles capable of



solubilizing up to 50 molecules of water per surfactant molecule.² Thus, a homogeneous mixture of 10% water in octane can be achieved with 0.1 M AOT. Presumably, AOT encases the water globules so that the octyl chains lie in the aprotic solvent and the ionic groups dip into the water.

Only a few sentences are necessary to summarize current thought on AOT-stabilized pools which have received much less attention than “normal” micelles in aqueous systems. AOT micelles in dry aprotic solvents are roughly spherical and monodisperse (single sized)³ and are characterized by distinct critical micelle concentrations.⁴ For example, the cmc and aggregation number of AOT in CCl_4 are 6×10^{-4} M and 17, respectively.^{5,6} In contrast, dodecylammonium propionate (the most widely known of the organic-soluble surfactants) lacks a cmc; the molecules assemble to form small ion clusters rather than true micelles.⁷ The cause of the remarkable water-solubilizing power of AOT is not understood, but we note in this regard that the *n*-octyl analogue of AOT does not effectively induce pool formation.⁸ Pool size varies with the $[\text{H}_2\text{O}]/[\text{AOT}]$ ratio; ratios of 2.2, 8.9, and 36 contain approximately 37, 410, and 6400 water molecules per aggregate.^{1,9} Both inorganic salts and organic compounds dissolve in the pools. Water-soluble fluorescent and spin label probes have helped determine the micropolarity and viscosity of the micelles as a function of size.¹⁰ We have shown that contracting the pool volume squeezes a spin label from the pool interior onto the micelle interface.¹⁰ Two mutually reactive molecules, dissolved separately in the water of two water pool solutions, are able to react with each other when the solutions are mixed.¹ Since reagent in one set of micelles can find reagent in the second set, water pools must merge, exchange contents, and reform at a rapid rate.

The work in the present article was prompted by what was originally considered a simple question: How does the pK_a of *p*-nitrophenol adsorbed inside water pools depend on pool size? As will be shown in the Discussion section, our results are intriguing and not as simple as we had hoped.

Experimental Section

Materials. *p*-Nitrophenol was recrystallized from chloroform and sublimed twice. *n*-Heptane (Aldrich Gold Label) was used without further purification. Fisher Aerosol OT (“100% dry” solid) was purified by adding 30 g to 60 mL of warm methanol. The mixture was then cooled in ice and centrifuged while cold. After discarding the sediment, we stirred the supernatant overnight with 3.0 g of Darco A-60 activated charcoal. The charcoal was separated by filtration, and the AOT was recovered by removing the solvent with a rotary evaporator and drying the residue over P_2O_5 for 12 h in an evacuated desiccator.

Procedure. AOT in *n*-heptane (0.02–0.20 M, 5 mL) was mixed with 0.20–1.0-mL aqueous buffer of known pH in a 10.00-mL volumetric flask. The solution was then diluted to the mark with *n*-heptane. A stoppered 10-mm cuvette was filled with 3.00 mL of AOT/ $\text{H}_2\text{O}/n$ -heptane and placed in the thermostated chamber (25.0 ± 0.1 °C) of a Cary 14 recording spectrophotometer. After waiting about 15 min for thermal equilibration, we traced the baseline, added to the cuvette 25 μL of 1.459×10^{-2} M *p*-nitrophenol in toluene, stirred the solution with a small glass rod, and ran a spectrum of the solution from 300–500 nm. No time-dependent absorbance changes were observed over a 3-h period. Beer’s law was obeyed at several wavelengths up to 3.7×10^{-4} M *p*-nitrophenol in the cuvette.

Results and Discussion

Let us begin by describing a typical water pool system consisting of 0.11 M AOT, 2.8 M water, and 1.2×10^{-4} M *p*-nitrophenol dissolved in *n*-heptane. The $[\text{H}_2\text{O}]/[\text{AOT}]$ ratio (hereafter designated *R*) equals 25, thus categorizing the pools as medium sized (*R* = 2–10 for small pools and 30–50 for large pools). Since AOT is present in 10^3 -fold excess over *p*-nitrophenol, and since the number of AOT molecules per micelle is much less than 10^2 , the pools in our typical solution generally contained no more than a single phenol molecule. We also provided the pools with an inorganic or imidazole buffer (0.001–0.20 M). Buffer concentrations reported in this paper are those of the aqueous solutions used to prepare the pool systems (see Experimental Section). This last comment is necessary because the buffer concentration within the water obviously exceeds that based on the entire heptane plus water volume.

It is not possible to insert a pH electrode into a pool and read the pH directly. One can only determine an operational pH, namely that of the water prior to mixing with the AOT/heptane. (A similar problem is encountered with pH-rate profiles of enzymes where the pH at the active site is unknown and the external pH must be used.) Our initial experiment involved a phosphate-buffered pool of *R* = 25.8 and pH 8.4. Judging from a lack of *p*-nitrophenolate absorbance at 420 nm, no phenolate was present in the pool. *p*-Nitrophenol in bulk water has a pK_a

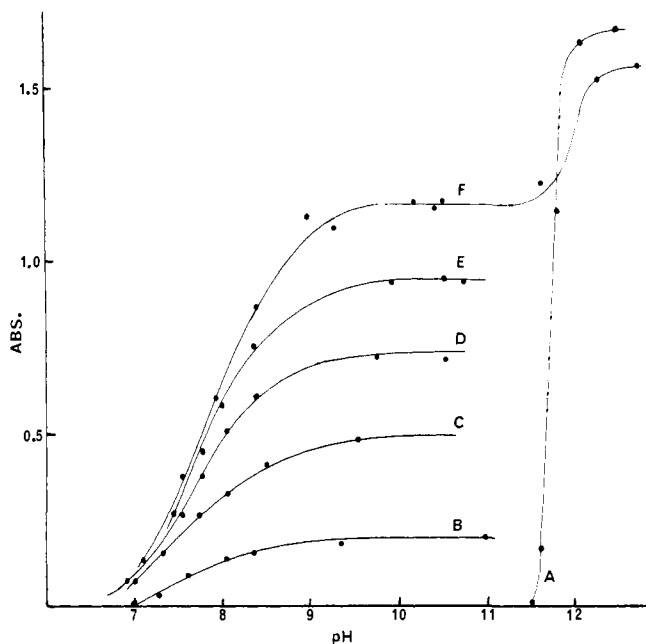


Figure 1. Plots of absorbance at 420 nm vs. pH of water pool in heptane at 25.0 °C ($R = 25.8$; $[AOT] = 0.108$ M; $[p\text{-nitrophenol}] = 1.22 \times 10^{-4}$ M). Plot A: aqueous NaOH. Plots B–F: 0.010, 0.025, 0.050, 0.100, and 0.201 M aqueous imidazole, respectively.

of 7.14 and is normally 95% ionized at pH 8.4. Resistance to ionization within the micelles is even more evident from studies of pools containing NaOH; *p*-nitrophenolate is not produced until the pH exceeds 11.5 (Figure 1A). This result cannot be attributed to neutralization of NaOH by acidic impurities in the AOT because such impurities seemed to be absent in a 1.0 M aqueous AOT solution. We conclude that the acidity of *p*-nitrophenol in a water pool system diminishes by 4.5 pK_a units.

There are three possible residence sites for the *p*-nitrophenol in the heptane/AOT/water: heptane, micelle interface, or water. Partitioning experiments led us to prefer strongly an interfacial or aqueous environment. Thus, partitioning of *p*-nitrophenol between mildly acidic water and heptane favors the water 100-fold. High salt concentrations in the water do not destroy the predilection for the aqueous phase: the partition coefficient between 2.0 M NaCl and heptane equals 75.

Buffering the pools ($R = 25.8$) with imidazole produced a surprising series of absorbance–pH curves (Figure 1B–F). *p*-Nitrophenol now ionizes nearer to its bulk-water pK_a of 7.14. But only a *fraction* of the total *p*-nitrophenol participates in this ionization equilibrium. For example, the flat pH 9.5–11 region for 0.010 M imidazole (Figure 1B) corresponds to only 12% phenolate. This percentage increases with the imidazole concentration (e.g., 70% at 0.20 M imidazole). Figure 1F shows that a profile rises toward *complete* ionization at pH >11.5. It is as if there are *two* species (of $pK_a \approx 7.7$ and 11.6) whose relative abundance depends on the imidazole concentration. When there is no imidazole (Figure 1A), *p*-nitrophenol exists solely in the form of the weaker acid.

We pause to consider the pK_a values of the “low pK_a ” member of the *p*-nitrophenol duo within the pools. These pK_a 's were determined from the data in Figure 1 by the usual plots¹¹ (Figure 2). The pK_a values, listed in Table I, increase uniformly from 7.56 to 7.92 as the imidazole buffer increases from 0.01 to 0.20 M. Although the variations appear to be real, they are small and will not be discussed further. We present Figure 2 and Table I merely to supply evidence that our complex pool system (containing five components!) is well-behaved with respect to a standard pK_a analysis.

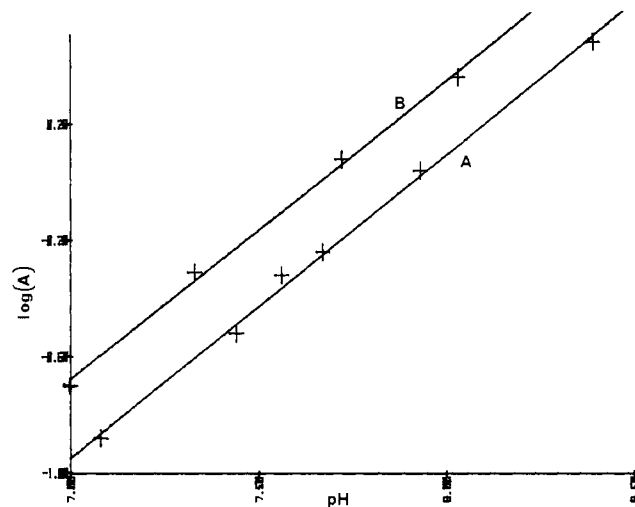


Figure 2. Spectrophotometric pK_a determination of *p*-nitrophenol in water pools ($R = 25.8$; $[AOT] = 0.108$ M; $[p\text{-nitrophenol}] = 1.22 \times 10^{-4}$ M). Parameter *A* represents the observed absorbance at 420 nm divided by the difference between the maximum possible and observed absorbances at 420 nm. Plot A: 0.025 M imidazole. Plot B: 0.201 M imidazole.

Table I. Dependence of the pK_a of *p*-Nitrophenol Inside Water Pools on the Aqueous Imidazole Concentration^a

[Imidazole], M	pK_a	[Imidazole], M	pK_a
0.010	7.56	0.100	7.78
0.025	7.66	0.201	7.92
0.050	7.73		

^a $[AOT] = 0.108$ M; $R = 25.8$; 25.0 °C.

Figure 3 deals with the dependency of *p*-nitrophenol ionization on pool size at constant $[AOT]$ and $[Im]$. Plots A, E, and F in Figure 3 (for which $R = 10.3, 25.8,$ and 36.1 at 0.11 M AOT and 0.20 M imidazole) reveal that the larger the pool the greater the percentage of the “low pK_a ” phenol. Thus, the small pool ($R = 10.3$) and the large pool ($R = 36.1$) titrate to 16 and 85% “low pK_a ” phenol, respectively. The remainder of the micellized phenol does not ionize until pH >11.5. Percents of the two types of phenol also vary with the total $[AOT]$ at constant R (Figure 3, plots B–E).

What is the nature of the two distinct *p*-nitrophenol species within the pool system? When an inorganic buffer (phosphate or NaOH) is present, only the more weakly acidic phenol ($pK_a \approx 11.6$) can be detected. This is reasonably explained by phenol adsorption at the heptane–water boundary (Figure 4). Since the phenolic hydroxy group is adjacent to anionic sulfonates of the AOT, ionization is impaired. Electrostatic inhibition of ionization is, of course, well-known outside the domain of water pools. For example, salicylate anion has a $pK_a = 13.82$ compared with a $pK_a = 9.98$ for phenol; the ortho carboxylate increases the pK_a of the neighboring phenolic proton by 3.84 units.

Perturbed ionization equilibria at protein surfaces, known for decades, do not in general rival the magnitude of those in our AOT system. For example, Klotz and Ayers¹² found that the dimethylamino group of an azo dye decreases in pK_a from 3.3 to 1.8 when the dye is attached to bovine serum albumin. The increased acidity reflects changes in the water structure at the protein surface. Tanford et al.¹³ classified the six phenolic groups of ribonuclease into two groups of three. One set ionizes normally and is presumably located near the surface; the other is buried in hydrophobic regions where the pK_a values exceed 11.5. In contrast to these two examples, *p*-nitrophenol in water pools is influenced primarily by electrostatic interactions. These interactions are far more potent than those in

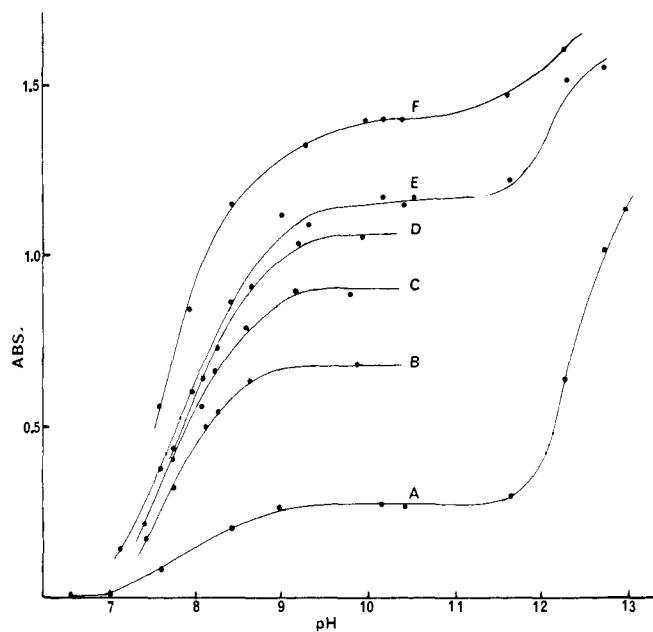


Figure 3. Absorbance at 420 nm vs. pH for water pools containing 1.22×10^{-4} M *p*-nitrophenol. The following three parameters are listed in order for each plot: *R*, [AOT], and [imidazole]. A: 10.3, 0.108 M, and 0.201 M. B: 25.8, 0.011 M, 0.193 M. C: 25.8, 0.022 M, 0.193 M. D: 25.8, 0.043 M, 0.193 M. E: 25.8, 0.108 M, 0.201 M. F: 36.1, 0.108 M, 0.201 M.

proteins or even "normal" aqueous micelles (which show alterations of dissociation constants of only 1–2 pK_a units).^{14–15}

The data in Figure 1B–F require that imidazole displace *p*-nitrophenol from the interface. The *p*-nitrophenol moves into the water phase, away from the sulfonates, where the pK_a assumes a more normal value (0.4–0.8 units larger than that in bulk water). Increasing the imidazole concentration increases the percent of dislodged phenol (Figure 1). A plot of [*p*-nitrophenolate] vs. [imidazole] at pH 10.0 and *R* = 25.8 displays saturation (curves downward), as would be expected from a competitive adsorption process. Only 50% of the interfacial *p*-nitrophenol is removed by a 28-fold excess of imidazole, indicating that the interface binds *p*-nitrophenol preferentially. This is reasonable because (1) the phenol possesses a more acidic proton with which it can hydrogen bond to the sulfonates and (2) the phenol molecule has amphiphilic properties (distinct hydrophilic and hydrophobic regions) and might be expected to gravitate toward hydrocarbon–water interfaces.

Studies by others have shown that imidazole complexes with AOT in CCl_4 .¹⁶ The association constant, determined by NMR, varied by a factor of 62 depending on whether the H-2 or H-5 proton of imidazole was observed. The difference was attributed to the nonidentical magnetic environments of the two protons. Although this explanation is clearly incorrect and something is amiss with the data, the association between imidazole and AOT supports our contention that imidazole and phenol compete for interfacial loci. Unlike imidazole, methanol (1.0 M), *n*-butyl alcohol (0.10 M), and *n*-butylamine hydrochloride (0.03 M) seem unable to replace *p*-nitrophenol at the interface.

Phenol incorporated into the water portion of the pools ionizes near pH 7.5. Yet, in the absence of imidazole, phenolate is not observed until the pH exceeds 11.5 (Figure 1A). We presume, therefore, that an unfavorable desorption equilibrium ($K = 10^{-4}$) precedes ionization in the pools. Relatively normal ionization within the medium-sized pools indicates an abundance of bulk water.

A constant imidazole concentration should displace a decreasing percentage of phenol as the pool size diminishes (there

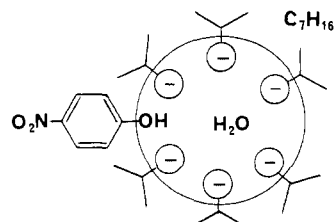


Figure 4. Schematic representation of *p*-nitrophenol adsorbed at the interface of an AOT-stabilized water pool.

is less free water to solubilize the phenol). This is found to be the case (Figures 3A, 3E, and 3F). When *R* = 36.1 ([AOT] = 0.11 M and [Im] = 0.20 M), almost 85% of the phenol exists in the "low pK_a " state. The value drops to 16% when there are only 10.3 molecules of water per AOT (other parameters being held constant). The pK_a of the solubilized phenol changes only from 7.93 to 7.74 as *R* increases from 10.3 to 36.1. Thus, according to a pK_a criterion, *p*-nitrophenol experiences much the same environment in pools of different sizes. Since only four or five water molecules are needed to solvate each AOT ion pair,^{2,17} all pools examined have sufficient "unbound" water to stabilize phenolic species. It would have been informative to investigate the extremely small pools (*R* ≤ 5), but phenol desorption is too unfavorable to permit such a study.

Liberation of phenol from the interface varies with the total [AOT] at constant *R* and [imidazole] (Figures 3B–E). For example, the proportion of aqueous phenol equals 42 and 70% at AOT concentrations of 0.011 and 0.11 M (*R* = 25.8). These results are readily understood if the pools enlarge as the [AOT] increases. It is sometimes assumed that pool size depends only on *R*, but we see that this is not strictly true. However, the assumption is probably reasonable over a small AOT concentration range.

We have discussed the multi-component pool system only qualitatively in the belief that such a description is easier to understand, if not more powerful, than one beset with complicated equations. Nonetheless, in conclusion, we should point out that the curves in Figure 1 can be duplicated precisely with the aid of eq 1:

$$A_{420} = \frac{[ArOH]_i \epsilon}{[1 + ([H^+]/K_a)] + [1 + 1/f([Im])]} \quad (1)$$

A_{420} represents the absorbance at 420 nm; $[ArOH]_i$ is the total phenol concentration in the cuvette; ϵ is the absorptivity at 420 nm; K_a is the ionization constant inside a water pool at a particular imidazole concentration; and $f([Im])$ is the ratio of total aqueous phenol to interfacial phenol equated to an experimentally determined logarithmic function of the imidazole concentration.¹⁸ At present, the dependence of *p*-nitrophenol ionization on pool size (Figure 3) defies a simple numerical analysis.

Acknowledgment. This investigation was supported by grants from the National Science Foundation and the National Institutes of Health.

References and Notes

- (1) F. M. Menger, J. A. Donohue, and R. F. Williams, *J. Am. Chem. Soc.*, **95**, 286 (1973).
- (2) W. K. Higuchi and J. Misra, *J. Pharm. Sci.*, **51**, 455 (1962).
- (3) J. B. Peri, *J. Colloid Interface Sci.*, **29**, 6 (1969).
- (4) The question of monodispersity and cmc range for AOT micelles is still not fully resolved. A. S. Kertes and H. Gutmann in "Surface and Colloid Science", Vol. 8, E. Matijevic, Ed., Wiley, New York, N.Y., 1976, p. 194.
- (5) S. Muto and K. Meguro, *Bull. Chem. Soc. Jpn.*, **46**, 1316 (1973).
- (6) K. Kon-No and A. Kitahara, *J. Colloid Interface Sci.*, **35**, 636 (1971).
- (7) N. Muller, *J. Phys. Chem.*, **79**, 287 (1975).

- (8) S. G. Frank and G. Zografi, *J. Colloid Interface Sci.*, **29**, 27 (1969).
 (9) See also H. Eicke and J. Rehak, *Helv. Chim. Acta*, **59**, 2883 (1976).
 (10) F. M. Menger, G. Saito, G. V. Sanzero, and J. R. Dodd, *J. Am. Chem. Soc.*, **97**, 909 (1975); M. Wong, J. K. Thomas, and M. Grätzel, *ibid.*, **98**, 2391 (1976).
 (11) A. Albert and E. P. Serjeant, "Ionization Constants of Acids and Bases", Wiley, New York, N.Y., 1962, p 73.
 (12) I. M. Klotz and J. Ayers, *J. Am. Chem. Soc.*, **79**, 4078 (1957).
 (13) C. Tanford, J. D. Hauenstein, and D. G. Rands, *J. Am. Chem. Soc.*, **77**, 6409 (1955).
 (14) E. H. Cordes and C. Giller, *Prog. Bioorg. Chem.*, **2**, 1 (1973).
 (15) F. M. Menger and J. L. Lynn, *J. Am. Chem. Soc.*, **97**, 948 (1975).
 (16) O. A. El Seoud and J. H. Fendler, *J. Chem. Soc., Faraday Trans. 1*, **71**, 452 (1975).
 (17) S. G. Frank, Y. Shaw, and N. C. Li, *J. Phys. Chem.*, **77**, 238 (1973).
 (18) $f[Im] = [Im](8.51 - 5.84 \log [Im])$.

Electrochemical and Solid State Studies of Phthalocyanine Thin Film Electrodes

Hiroyasu Tachikawa and Larry R. Faulkner*¹

Contribution from the Department of Chemistry, University of Illinois, Urbana, Illinois 61801. Received December 16, 1977

Abstract: Electrochemical studies have been made of phthalocyanine surfaces. The electrodes were fabricated by evaporating 70 Å of chromium, 300 Å of gold, and ~3000 Å of a phthalocyanine, in sequence, onto a glass substrate in vacuo. Metal-free, zinc, iron(II), and copper phthalocyanines (H₂Pc, ZnPc, FePc, and CuPc) were examined. ZnPc and FePc electrodes showed a capacity for nearly reversible charge transfer reactions on a cyclic voltammetric time scale, and this Faradaic activity could be assigned to the phthalocyanine surfaces themselves. Parallel experiments with gold/phthalocyanine/gold sandwich devices highlighted the importance of water and oxygen for introducing appreciable electronic conductivity into the phthalocyanine phases. These ambient effects on the bulk phases were mirrored in the voltammetric responses of the phthalocyanine electrodes. ZnPc and FePc surfaces could not efficiently mediate electrode reactions (including O₂ reduction) that occurred on Au at potentials more negative than 0.0 V vs. SCE, whereas reactions in the positive region proceeded readily. Several of the inhibited reactions could be photoassisted on ZnPc. The results are generally in accord with a view of the phthalocyanines as fairly well behaved p-type semiconductor electrodes having flat-band conditions near 0.0 V vs. SCE.

Electrochemical reactions at chemically modified surfaces have attracted much attention lately, because they may be useful in promoting catalytic or selective electrode processes.²⁻²² Surface-linked chromophores have also been used to extend the spectral responses of semiconductor photoelectrodes to longer wavelengths.¹³ Besides serving these practical ends, surface-modified electrodes represent some interesting new tools for fundamental studies of electron-transfer reactions.

In most published work along this line, elegant chemical steps have been used to bond electron or photon mediators to a surface at roughly monolayer coverage. An alternative approach to new and chemically interesting electrode surfaces is to enable Faradaic reactions to occur directly on molecular solids. This option has not been explored to any great extent, because the bulk conductivities of such materials are usually low, hence they cannot be used for electrodes of conventional dimensions. Molecular phases with metallic conductivity provide the exceptions to this rule, and recent work by Nowack et al. with polymeric sulfur nitride, (SN)_x, has opened the way to further research with massive molecular electrodes made from highly conductive materials.²³

Other substances can be fabricated into useful electrodes by employing thin film technology. A thickness on the order of 1000 Å deposited over a metallic conductor can provide a current path of sufficiently low resistance, even with bulk resistivities in the overlayer as high as 10⁸ ohm cm. Our concern here is with electrodes of this type made from various phthalocyanines.

The phthalocyanines have received much attention in electrochemistry since 1964, when Jasinski reported that several of them could catalyze the electroreduction of oxygen in aqueous media.^{24,25} Electrodes of many types have been fabricated.²⁴⁻⁴³ Powdered carbon or metal has been coated with the phthalocyanines by chemical vapor deposition, solvent

evaporation, and electrophoretic deposition. These same powders have also been pressed with crystalline phthalocyanines into composite electrodes. Bulk metal surfaces have been coated by solvent evaporation, by adsorption from solution, and, in relatively few cases, by deposition of the phthalocyanine by evaporation in vacuo. Virtually all of the reported studies were devoted to the catalysis of oxygen's electroreduction. Catalysis was frequently observed, but in most of this work it has been difficult to discern whether the Faradaic process actually occurs on the phthalocyanine or, instead, takes place on the conducting support while being facilitated by ancillary heterogeneous reactions on nearby phthalocyanine surfaces.^{31,41}

However, several recent investigations have given strong indications that the phthalocyanine surfaces are indeed capable of Faradaic reactions. Appleby and Savy have made careful studies of the kinetics of O₂ reduction,^{39,41} and they have observed markedly different pH dependences for Tafel slopes recorded for coated and uncoated carbon powders. These authors have also done very extensive spectroscopic and electrochemical work with thin films of phthalocyanines on planar substrates, and they have discussed detailed hypotheses about the chemical basis for the observed electrocatalysis.^{37,39,41} Alferov and Sevast'yanov observed photoinduced reduction of O₂ on several phthalocyanines that were evaporated to 100-1000 Å thicknesses on polished graphite.³⁶ The origin of the photoeffect was not explained in detail, but it may manifest semiconductor-based photoelectrochemical properties of the phthalocyanines. More recently, Meshitsuka and Tamura have observed photoinduced oxidation of oxalate on 10 000 Å thick films of CuPc deposited over Pt.⁴⁰ Their results could be quantitatively interpreted in terms of Faradaic activity on the outer surface of CuPc, which behaved like an intrinsic semiconductor.

Our interest here is with the more general electrochemical